

# Crystal Structure of the Extended-Spectrum $\beta$ -Lactamase PER-2 and Insights into the Role of Specific Residues in the Interaction with $\beta$ -Lactams and $\beta$ -Lactamase Inhibitors

Melina Ruggiero,<sup>a</sup> Frédéric Kerff,<sup>b</sup> Raphaël Herman,<sup>b</sup> Frédéric Sapunari,<sup>b</sup> Moreno Galleni,<sup>b</sup> Gabriel Gutkind,<sup>a</sup> Paulette Charlier,<sup>b</sup> Eric Sauvage,<sup>b</sup> Pablo Power<sup>a</sup>

Laboratorio de Resistencia Bacteriana, Facultad de Farmacia y Bioquímica, Universidad de Buenos Aires, Buenos Aires, Argentina<sup>a</sup>; Centre d'Ingénierie des Protéines, Université de Liège, Liège, Belgium<sup>b</sup>

PER-2 belongs to a small (7 members to date) group of extended-spectrum  $\beta$ -lactamases. It has 88% amino acid identity with PER-1 and both display high catalytic efficiencies toward most  $\beta$ -lactams. In this study, we determined the X-ray structure of PER-2 at 2.20 Å and evaluated the possible role of several residues in the structure and activity toward  $\beta$ -lactams and mechanism-based inhibitors. PER-2 is defined by the presence of a singular *trans* bond between residues 166 to 167, which generates an inverted  $\Omega$  loop, an expanded fold of this domain that results in a wide active site cavity that allows for efficient hydrolysis of antibiotics like the oxyimino-cephalosporins, and a series of exclusive interactions between residues not frequently involved in the stabilization of the active site in other class A  $\beta$ -lactamases. PER  $\beta$ -lactamases might be included within a cluster of evolutionarily related enzymes harboring the conserved residues Asp136 and Asn179. Other signature residues that define these enzymes seem to be Gln69, Arg220, Thr237, and probably Arg/Lys240A ("A" indicates an insertion according to Ambler's scheme for residue numbering in PER  $\beta$ -lactamases), with structurally important roles in the stabilization of the active site and proper orientation of catalytic water molecules, among others. We propose, supported by simulated models of PER-2 in combination with different  $\beta$ -lactams, the presence of a hydrogen-bond network connecting Ser70-Gln69-water-Thr237-Arg220 that might be important for the proper activity and inhibition of the enzyme. Therefore, we expect that mutations occurring in these positions will have impacts on the overall hydrolytic behavior.

Class A  $\beta$ -lactamases (EC 3.5.2.6) are the most prevalent enzymes conferring high-level resistance to  $\beta$ -lactam antibiotics among human pathogens. This molecular group comprises enzymes that efficiently hydrolyze amino-penicillins and older (first- and second-generation) cephalosporins and are inhibited, to different extents, by mechanism-based  $\beta$ -lactamase inhibitors like clavulanic acid, tazobactam, and sulbactam. They also encompass several extended-spectrum  $\beta$ -lactamases (ESBL) that widen their range of hydrolysable drugs to newer  $\beta$ -lactams such as the oxyimino-cephalosporins like cefotaxime (CTX) and ceftazidime (CAZ) (1, 2).

Within the vast family of class A  $\beta$ -lactamases, PER  $\beta$ -lactamases are a unique group of ESBL that are circumscribed to few locations around the world (2). PER-1 was first recognized in a clinical bacterial strain isolated from a hospitalized patient in France; it was more recently detected among other microorganisms in a few other countries, especially *Pseudomonas aeruginosa* and *Acinetobacter baumannii* (2–6). Other closely related enzymes are PER-3, -4, -5, and -7 (2, 7).

PER-2 was detected for the first time in a *Proteus mirabilis* strain isolated in Argentina in 1989, although it was at that time named ARG-1 (8). Nevertheless, the gene sequence located on a transferable plasmid was described as *bla*<sub>PER-2</sub> in a ceftibuten-resistant *Salmonella enterica* serovar Typhimurium isolate (9).

Since it was first reported, PER-2 has been found in other species and countries, although it is particularly prevalent in Argentina and Uruguay (2) and accounts for up to 10% and 5% of the oxyimino-cephalosporin resistance in *Klebsiella pneumoniae* and *Escherichia coli*, respectively (10). PER-6, encoded in the chromosome of an environmental *Aeromonas allosaccharophila* isolate, is

the only variant close to PER-2 that may elucidate the evolutionary path of PER  $\beta$ -lactamases (11).

PER-2 shares 88% amino acid sequence identity with mature PER-1 and both of them display high catalytic efficiencies ( $k_{cat}/K_m$ ) toward most  $\beta$ -lactams, generally characterized by similar values for both ceftazidime and cefotaxime, although for PER-2 the values seem to be nearly one order of magnitude higher than those for PER-1 (12, 13). PER-2 is also strongly inhibited by mechanism-based inhibitors such as clavulanate and tazobactam (12).

The X-ray structure of PER-1 has been solved (14), and the roles of different residues have also been studied for this variant (13, 15).

In this study, we determined the X-ray structure of PER-2 at 2.2 Å and evaluated the possible roles of several key residues in the structure and activity of  $\beta$ -lactams and mechanism-based  $\beta$ -lactamase inhibitors.

## MATERIALS AND METHODS

**Strains and plasmids.** *Escherichia coli* TC9 is a transconjugant clone harboring the pCf587 plasmid, used as the source of the *bla*<sub>PER-2</sub> gene (12). *Escherichia coli* Top10F' (Invitrogen, USA) and *Escherichia coli*

Received 13 January 2014 Returned for modification 16 February 2014

Accepted 20 July 2014

Published ahead of print 28 July 2014

Address correspondence to Pablo Power, ppower@ffyba.uba.ar.

Copyright © 2014, American Society for Microbiology. All Rights Reserved.

doi:10.1128/AAC.00089-14

BL21(DE3) (Novagen, USA) were hosts for transformation experiments. Plasmid vectors pGEM-T Easy vector (Promega, USA) and kanamycin-resistant pET28a(+) (Novagen, Germany) were used for routine cloning experiments and for enzyme overproduction, respectively.

**Molecular biology techniques.** Plasmid DNA (pTC9) was extracted using the methodology described by Hansen and Olsen (16). The PER-2-encoding gene was amplified by PCR from plasmid pTC9, using 1 U *Pfu* DNA polymerase (Promega, USA) and 0.4  $\mu$ M PER2-BamF1 (5'-TCAT TTGTAGGATCCGCCCAATC-3') and PER2-SacR1 primers (5'-CTTTA AGAGCTCGCTTAGATAGTG-3'), containing the BamHI and SacI restriction sites, respectively (underlined in the sequences), designed for allowing the cloning of the mature PER-2 coding sequence. The PCR product was first ligated in a pGEM-T Easy vector; the insert was sequenced for verification of the identity of the *bla*<sub>PER-2</sub> gene and generated restriction sites, as well as the absence of aberrant nucleotides. The resulting recombinant plasmid (pGEM-T/*bla*<sub>PER-2</sub>) was then digested with BamHI and SacI, and the released insert was subsequently purified and cloned in the BamHI-SacI sites of a pET28a(+) vector. The ligation mixture was used to first transform *E. coli* Top10F' competent cells, and after selection of recombinant clones, a second transformation was performed in *E. coli* BL21(DE3) competent cells in LB plates supplemented with 30  $\mu$ g/ml kanamycin. Selected positive recombinant clones were sequenced for confirming the identity of the *bla*<sub>PER-2</sub> gene, and from them the recombinant clone *E. coli* BL-PER-2-BS harboring the pET/*bla*<sub>PER-2</sub> plasmid was used for protein expression experiments. The resulting construct expresses a fusion peptide including a mature PER-2-encoding gene plus an additional sequence containing a 6 $\times$ His tag and a thrombin cleavage site. DNA sequences were determined at the GIGA facilities (Liege, Belgium). Nucleotide and amino acid sequence analyses were performed by NCBI (<http://www.ncbi.nlm.nih.gov/>) and ExPASy (<http://www.expasy.org/>) analysis tools.

**PER-2 production and purification.** Overnight cultures of recombinant *E. coli* BL-PER-2-BS (harboring pET/*bla*<sub>PER-2</sub> plasmid construction) were diluted (1/50) in 2 liters LB containing 30  $\mu$ g/ml kanamycin and grown at 37°C to ca. 0.8 optical density (OD) units ( $\lambda$ , 600 nm). In order to induce  $\beta$ -lactamase expression, 0.4 mM IPTG (isopropyl- $\beta$ -D-thiogalactopyranoside) was added and cultures were grown at 37°C for 3 h. After centrifugation at 8,000 rpm (4°C) in a Sorvall RC-5C, cells were resuspended in sodium phosphate buffer (20 mM [pH 8.0]) and supplemented with 3 U/ml Benzonase (Sigma-Aldrich, USA), and crude extracts were obtained by mechanic disruption in an EmulsiFlex-C3 homogenizer (Avestin Europe GmbH, Germany) after three passages at 1,500 bar. After clarification by centrifugation at 12,000 rpm (4°C), clear supernatants containing the PER-2 fusion peptide were filtered by 1.6- and 0.45- $\mu$ m-pore-size membranes prior to purification. Clear supernatants were loaded onto 5-ml HisTrap HP affinity columns (GE Healthcare Life Sciences, USA), connected to an ÄKTA purifier (GE Healthcare, Uppsala, Sweden), and equilibrated with buffer A (20 mM sodium phosphate buffer [pH 8.0]) and 0.5 M sodium chloride. The column was extensively washed to remove unbound proteins, and  $\beta$ -lactamases were eluted with a linear gradient (0 to 100% at a 2 ml/min flow rate) of buffer B (buffer A plus 500 mM imidazole [pH 8.0]). Eluted fractions were screened for  $\beta$ -lactamase activity during purification by an iodometric system using 500  $\mu$ g/ml ampicillin as the substrate (17), followed by SDS-PAGE in 12% polyacrylamide gels. Active fractions were dialyzed against buffer A2 (20 mM Tris-HCl buffer [pH 8.0]), and the His tag was eliminated by thrombin digestion (16 h at 25°C), using 5 U thrombin (Novagen, USA) per mg protein for complete proteolysis. The digestion mixture was then loaded onto 1-ml HisTrap HP columns (GE Healthcare Life Sciences, USA) equilibrated in buffer A2, and the pure mature PER-2 was separated from the digested histidine-tagged peptide eluted with buffer B2 (buffer A2 plus 500 mM imidazole [pH 8.0]). Protein concentration and purity were determined by the bicinchoninic acid (BCA) protein quantitation assay (Pierce, Rockford, IL, US) using bovine serum albumin as the standard, and by densitometry analysis on 15% SDS-PAGE gels, respectively. Puri-

fied protein was subjected to automatic Edman degradation for the N-terminal amino acid sequence determination using an Applied Biosystems 492 protein sequencer (PerkinElmer, Waltham, MA, USA).

**Crystallization.** Crystals were grown at 20°C using the hanging drop vapor diffusion method with drops containing 2.5  $\mu$ l of PER-2 solution (3.5 mg/ml) and 1  $\mu$ l 0.1 M HEPES in 1.5 M sodium citrate buffer (pH 7.5), equilibrated against 1 ml of the latter solution at 20°C.

**Data collection and phasing.** Data were collected on a Pilatus 6-M Dectris detector at a wavelength of 0.98011 Å on a Proxima 1 beamline at the Soleil Synchrotron (Saint Aubin, France). X-ray diffraction experiments were carried out under cryogenic conditions (100 K) after transferring the crystals into cryoprotectant solution containing 1.8 M ammonium sulfate and 45% (vol/vol) glycerol. Indexing and integration were carried out using XDS (18), and the scaling of the intensity data was accomplished with XSCALE (19).

**Model building and refinement.** Refinement of the model was carried out using REFMAC5 (20), TLS (21), and Coot (22). Model visualization and representation were performed with PyMOL ([www.pymol.org](http://www.pymol.org)) (23).

**Simulated modeling of PER-2 in complex with oxyimino-cephalosporins and clavulanate.** The X-ray structure of PER-2 was used to model acyl-enzyme structures with ceftazidime, cefotaxime, and clavulanic acid. The structures with PDB numbers 2ZQD (TOHO-1 in complex with ceftazidime), 1IYO (TOHO-1 in complex with cefotaxime [24]), and 2HOT (SHV-1 in complex with clavulanic acid [25]) were used for initial positioning of each ligand in the PER-2 structure. Simulation structures were energy minimized with the program YASARA (26), using a standard protocol consisting of a steepest-descent minimization followed by simulated annealing of the ligand and protein side chains. PER-2 backbone atoms were kept fixed during the whole procedure. Simulation parameters consisted of the use of a Yasara2 force field (27), a cutoff distance of 7.86 Å, particle mesh Ewald (PME) long-range electrostatics (28), periodic boundary conditions, and a water-filled simulation cell.

**Protein structure accession number.** The structure of PER-2 was refined to 2.2 Å and deposited at the Protein Data Bank under the accession number 4D2O.

## RESULTS AND DISCUSSION

**Structure determination of PER-2  $\beta$ -lactamase.** The structure of PER-2 was obtained at a resolution of 2.2 Å. Main data and refinement statistics are given in Table 1.

The refined structure consists of two monomers per asymmetric unit. Monomer A includes 280 amino acids of mature  $\beta$ -lactamase, from Ala24 to Val297; monomer B contains 278 residues, from Ser26 to Val297. The structure is solvated by 152 ordered water molecules.

The electron density map is well defined along the main chain of both monomers except for the region covering residues Leu103-Gln103A-Asn103B in chain A ("A" and "B" indicate insertions according to Ambler's scheme for residue numbering in PER  $\beta$ -lactamases) and the last C-terminal residues (Ser298-Pro299-Asp300) in both chains.

The root mean square (RMS) deviation between the equivalent C $\alpha$  atoms in both monomers is 0.64 Å, and no significant differences were found between the two active sites. Due to this observation, the following discussion refers to both monomers unless otherwise noted.

**PER-2 and PER-1 share overall structure and main structural features within the active site.** The overall fold of the native PER-2  $\beta$ -lactamase is similar to that of the previously reported PER-1 structure (PDB 1E25) (14), displaying an RMS deviation (RMSD) of 0.619 Å between them.

As in other class A  $\beta$ -lactamases, the active site motifs are located in the interface between the all- $\alpha$  and  $\alpha/\beta$  domains. They are

**TABLE 1** Data collection, diffraction, and phasing statistics for native PER-2  $\beta$ -lactamase

Crystal parameter(s) <sup>a</sup>	Native PER-2 data <sup>b</sup>
PDB code	4D2O
Data collection:	
Space group	P 1 2 1
Cell parameters	
<i>a</i> , <i>b</i> , <i>c</i> (Å)	41.48, 83.88, 68.94
$\alpha$ , $\beta$ , $\gamma$ (°)	90.00, 103.92, 90.00
Subunits/ASU	2
Resolution range (Å)	41.94–2.20 (2.32–2.20)
Total no. of reflections	159,256
No. of unique reflections	23,354 (3,390)
<i>R</i> <sub>merge</sub> (%)	14.5 (65.0)
Redundancy	6.8 (6.9)
Completeness (%)	100 (100)
Mean <i>I</i> / $\sigma$ ( <i>I</i> )	10.5 (3.1)
Refinement	
Resolution range	33.46–2.20
No. of protein atoms	4,407
No. of water molecules	152
<i>R</i> <sub>cryst</sub> (%)	19.44
<i>R</i> <sub>free</sub> (%)	23.97
RMS deviations from ideal stereochemistry:	
Bond lengths (Å)	0.013
Bond angles (°)	1.619
Planes (Å)	0.007
Chiral center restraint (Å <sup>3</sup> )	0.105
Mean B factor (all atoms) (Å <sup>2</sup> )	29.2
Ramachandran plot	
Favored region (%)	97.4
Allowed regions (%)	2.6
Outlier regions (%)	0.0

<sup>a</sup> ASU, asymmetric unit; RMS, root mean square.

<sup>b</sup> Data in parentheses are statistics for the highest-resolution shell.

defined as Ser70-Val71-Phe72-Lys73 (motif 1, carrying the nucleophile serine), Ser130-Asp131-Asn132 (motif 2, in the loop between  $\alpha$ 4 and  $\alpha$ 5), Lys234-Thr235-Gly236 (motif 3, on strand  $\beta$ 3), and the 14-residue-long  $\Omega$ -loop, from Ala164 to Asn179 (Fig. 1).

Compared to other class A  $\beta$ -lactamases, PER-2 has three insertions along its sequence, (i) Gln103A-Asn103B and (ii) Gln112A-Gly112B (both located at the bottom of the all- $\alpha$  domain, as part of a long fold connecting helices  $\alpha$ 2 and  $\alpha$ , and facing the  $\Omega$  loop), and (iii) Arg240A-Ala240B-Gly240C-Lys240D, an insertion that creates an enlarged loop just after the KTG conserved motif (Fig. 2a).

The insertion Gln103A-Asn103B creates a new fold that seems to be stabilized by hydrogen bonds between the Ser106 backbone and probably some rotamers of Gln103A, which differs from the conserved bend (Val103-Asn106) in other class A  $\beta$ -lactamases like CTX-M (24).

The most relevant structural trait observed in PER-2 (and also PER-1 [14]) is the presence of an expanded active site, which contributes to facilitated access of bulkier molecules such as the oxymino-cephalosporins. This is achieved by two main features, a unique “inverted”  $\Omega$  loop (Fig. 2a), whose configuration is the result of a *trans* bond between Glu166 and Ala167 (instead of the normally occurring *cis* bond in all the other class A  $\beta$ -lactamases),

and an expanded loop between the  $\beta$ 3 and  $\beta$ 4 strands (named the  $\beta$ 3- $\beta$ 4 loop), resulting from the insertion of four residues after the KTG motif that enlarge the active site entrance up to 12.2 Å (compared to ca. 6.5 Å in other class A  $\beta$ -lactamases) (Fig. 2b).

The overall structure of the  $\Omega$  loop is stabilized by hydrogen bonds between the carboxylate’s oxygen of Asp136 (replacing the highly conserved Asn136 in other class A  $\beta$ -lactamases) and main chain nitrogen atoms of Glu166 (2.9 Å) and Ala167 (3.0 Å) (Fig. 2c) and by additional bonds between Ala164 and Asn179, the initial and final residues of the  $\Omega$  loop.

The positioning and orientation of side chains of important residues such as Ser70, Lys73, Ser130, Glu166, and Thr237 are equivalent to those of other class A  $\beta$ -lactamases (Fig. 3a and b). These findings, and the fact that C $\alpha$  RMSD values of the conserved motifs of PER-2 are comparable to those of other class A  $\beta$ -lactamases, indicate that there is conservation in the overall structure of the active site (Table 2).

We noted the presence of water molecules associated with the oxyanion hole (Wat14 in monomer A and Wat113 in monomer B) (Fig. 3a), located 3.29 Å and 2.85 Å from the Ser70N and Thr237N of the oxyanion hole, respectively (“N” in the residue numbers stands for the main chain nitrogen atom defining the oxyanion hole) (Fig. 3b), in agreement with the proposed water molecule found at the PER-1 active site (Wat2153) (14) and in other class A  $\beta$ -lactamases as well (for reference, see PDB molecules 1BTL [TEM-1], 1SHV [SHV-1], 1IYS [TOHO-1], and 3DW0 [KPC-2]).

On the other hand, the presence of a deacylating water is not clearly evidenced; no electron density is apparent at the equivalent position of the deacylating water Wat2075 in PER-1 (14).

**Additional structural features probably involved in the stabilization of the active site of PER-2.** We observed several features at the active site environment of PER-2 not previously evaluated for PER-1 (some of these are shown in Fig. 3a).

A water molecule (Wat52) at the entrance of the catalytic site stabilizes the sharp  $\beta$ 3- $\beta$ 4 fold through hydrogen bonds with residues of the  $\Omega$  loop, probably avoiding possible clashes between both domains.

Some of the possible rotamers of Arg240A (at the end of the  $\beta$ 3 strand, replaced by Lys240A in PER-1) might interact with Asp173 (at the  $\Omega$  loop), probably modulating the rate by which  $\beta$ -lactams gain access to the active site (see below).

The benzyl side chain of Phe72 rotates ca. 45° relative to the same residue in other class A  $\beta$ -lactamases like TEM and SHV (CTX-M enzymes contain a serine at position 72), creating a hydrophobic environment (due to repulsion between Phe72 and Phe139) that might have an impact on the interaction with some antibiotics. Alternatively, Met169 (replaced by leucine in other class A  $\beta$ -lactamases) might induce the Phe72 rotation by non-hydrogen bond interactions (29, 30).

**Gln69, Arg220, and Thr237 participate in a hydrogen bond network important for the stabilization of the active site.** Previous studies have already scrutinized the role of different residues in the ability of PER-1 to hydrolyze third-generation cephalosporins (13, 15). The influence of other residues in the inhibition by mechanism-based inhibitors has been also assessed (31).

Glutamine 69 has been proposed as the second ligand for the deacylating water for PER-1 (14), homologous to Asn170 in the other class A  $\beta$ -lactamases (32, 33). We observed that the Gln69 side chain in PER-2 seems to occupy space equivalent to that of the highly conserved Asn170 from other class A  $\beta$ -lactamases, like

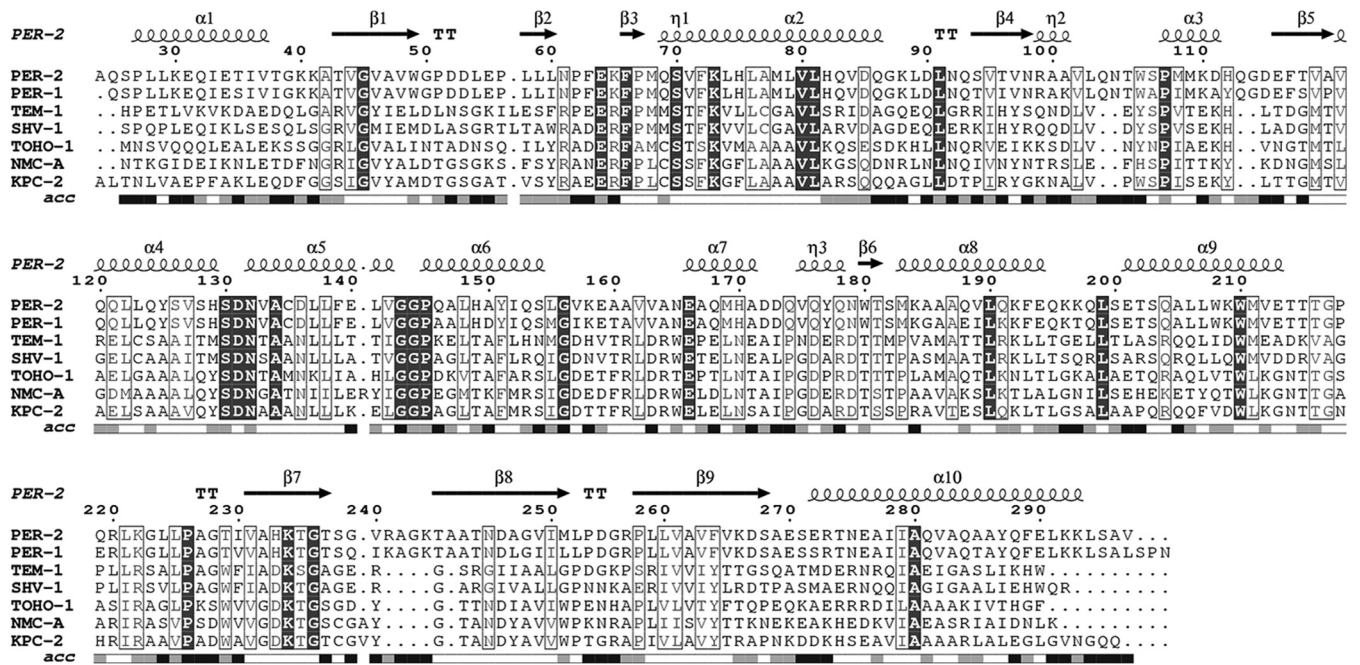


FIG 1 Amino acid sequence alignment of PER-2 and other class A  $\beta$ -lactamases for which the crystallographic structure has been determined using the Ambler residue numbering. Location of  $\alpha$  helices and  $\beta$  sheets is indicated in the upper side (taken from the PDB file), and relative solvent accessibility in the bottom (black, highly accessible; gray, poorly accessible; white, hidden or inaccessible). ESPript (<http://esprict.ibcp.fr/ESPript/ESPript/>) was used to make the figure.

TOHO-1. This is partly due to the fact that Asn170 is replaced by His170 in PER enzymes, and its position relative to the active site environment is dramatically modified as a result of the peculiar  $\Omega$  loop (C $\alpha$  of His170 is displaced between 6.5 and 7.3 Å away from the active site).

It is known that in class A  $\beta$ -lactamases like TEM and SHV variants, Arg244 seems to play an important role in substrate and inhibitor binding (34–36). This role seems to be fulfilled in CTX-M  $\beta$ -lactamases by Arg276 (37). In other class A  $\beta$ -lactamases like the *Streptomyces albus* G  $\beta$ -lactamase or KPC-2 and NMC-A carbapenemases (PDB entries 1BSG, 3DW0, and 1BUE, respectively) (38), an arginine residue at position 220 was observed at the  $\beta$ 4 strand whose side-chain guanidinium group occupies a position equivalent to that of the lateral residue of Arg244/Arg276 in the mentioned class A  $\beta$ -lactamases. For some of these enzymes, Arg220 was evaluated regarding its influence on substrate and inhibitor binding, giving this residue role similar to that of Arg244 in TEM/SHV variants (39, 40).

For PER-1, the same role has been suggested, according to an Arg220Leu mutant showing modified kinetic parameters toward some  $\beta$ -lactams (13).

We have structural evidence demonstrating that Arg220 in PER-2 allows the creation of a network of interactions with neighboring residues that differs from the associations observed in  $\beta$ -lactamases harboring Arg244/276. As shown in Fig. 3c, the guanidinium group of Arg220 hydrogen bonds with Thr237 (2.7 and 2.8 Å), Asn245 (3.1 Å), Glu276 (2.7 Å), and Gly236 (3.2 Å), and additional interactions occur between Arg220 and Gly217, Lys222, and Gly223 (through hydrogen bonds) and between the Arg220 side chain and Asp246 through nonpolar interaction. In TEM-1, SHV-1, and TOHO-1, fewer polar interactions occur be-

tween Arg244/Arg276 and close residues (not shown), and these differences might partially explain the higher catalytic efficiencies of PER-2 toward some antibiotics.

Another striking difference between PER  $\beta$ -lactamases and the vast majority of class A enzymes is the presence of a threonine at position 237. From the structure of PER-2, we confirmed the possible importance of Thr237 for connecting essential residues of the active site with Arg220 through a not previously reported network of hydrogen bonds (comprising Ser70-Gln69-Wat14-Thr237-Arg220), in which Thr237 might serve as a stake connecting both domains (Fig. 3b), and additional interactions between Arg220 and both Thr244 and Glu276 that could further improve the overall stabilization of the structure. In fact, both Arg220 and Thr237 seem to contribute to the topological adjustment of the oxyanion pocket, as also suggested for other class A  $\beta$ -lactamases (13, 41). The hydroxyl group of Thr237 is also important for interaction with the substrate, providing the possibility for an additional hydrogen bond with the substrate carboxylate group, as described below.

**Simulated acyl-enzyme models of PER-2 provide clues about interactions with oxymino-cephalosporins and inhibitors.** As seen in Fig. 4a, a simulated acyl-enzyme model of the PER-2 structure in complex with cefotaxime (generated using the TOHO-1/cefotaxime structure, PDB 1IYO [24]) indicated that cefotaxime is positioned in the binding site of PER-2 through hydrogen bonds with Gln69, Ser130, Asn132, Glu166, Thr235, and Thr237. Altogether, these interactions with the cefotaxime molecule might support the efficient hydrolysis of the oxymino-cephalosporins by PER  $\beta$ -lactamases (11, 12, 15).

As discussed, Thr237 might be involved in critical networking by stabilizing the active site and the  $\beta$ 3 strand and acting as

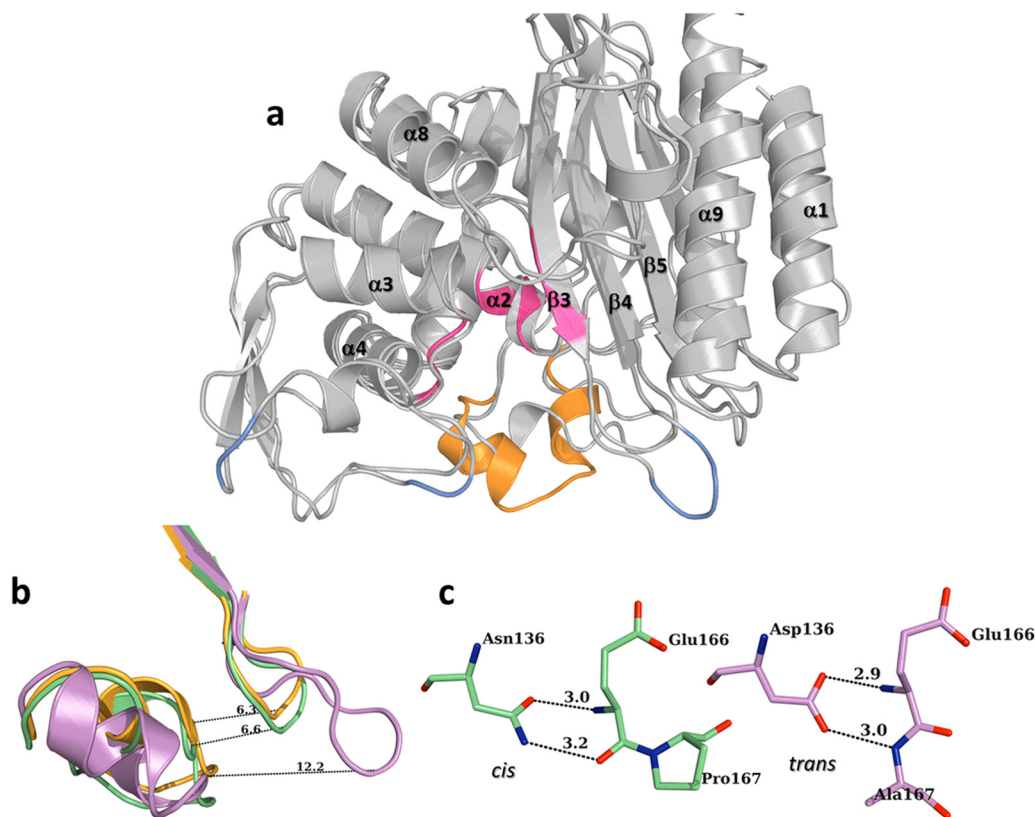


**FIG 2** (a) Overall structure of PER-2  $\beta$ -lactamase, showing the location of the main motifs of the active site (pink), the unique  $\Omega$  loop (orange), and the three insertions (compared to TEM-1; pale blue). (b) Detail of the four-residue insertion in PER-2 (pink) that creates an expanded loop between  $\beta$ 3 and  $\beta$ 4 strands, widening the active site entrance (orange, TEM-1; green, TOHO-1). (c) Comparison between the singular *trans* bond between Glu166-Ala167 and hydrogen bonds with Asp136 in PER-2 (pink) and the normally *cis* bond between Glu166-Pro167 (and hydrogen bonds with Asn136) found in other class A  $\beta$ -lactamases like TOHO-1 (green). All distances are in angstroms ( $\text{\AA}$ ).

a connector of the  $\beta$ -lactam molecule with Arg220, the other essential residue in this network. From the model, we propose that Arg240A (present in the enlarged loop connecting  $\beta$ 3 and  $\beta$ 4 strands), is involved in some stage during the entrance of cefotaxime into the active site, probably assisted by Asp173. In TOHO-1 and other class A  $\beta$ -lactamases, Asp240 (at a position equivalent to that of Arg240A in PER-2) participates in the interaction with the aminothiazole ring of cefotaxime during entrance to the active site (24, 42), although we do not have evidence of such an interaction between cefotaxime and Arg240A in PER-2.

A similar scenario is obtained for the acylated PER-2 model in complex with ceftazidime (Fig. 4b), using the TOHO-1/ceftazidime structure (2ZQD). The model predicts that the existence of an expanded catalytic cavity might in fact allow a suitable accommodation of ceftazidime through interactions with Gln69, Ser130, Asn132, Glu166, Thr235, and Thr237.

Additional interactions between ceftazidime and other residues were also detected in comparison to other  $\beta$ -lactamases. For example, Asp173, Gln176, and Arg240A seem to be closer to the ceftazidime molecule and might have some role in the accommodation or entrance of the molecule. In addition, the dihydrothiazine ring in the ceftazidime molecule allows van der Waals interactions with Trp105, and the long carboxy-propoxyimino group might establish additional polar interactions with Thr237 and

Ser238 carbonyl oxygen atoms, probably due to the increased flexibility in the PER-2  $\beta$ 3 strand. Supporting this hypothesis, Ser238 is involved in the efficient hydrolysis of ceftazidime in TEM/SHV ESBLs by advantageous interactions with Ser238 and Asn170 (the spatial equivalent to Gln69 in PER enzymes) (43). In CTX-M  $\beta$ -lactamases, the low hydrolysis rate of ceftazidime might be explained by unfavorable interactions or even repulsion between active-site residues and the ceftazidime carboxy-propoxyimino group in the C7 $\beta$  side chain (44).

Therefore, the interactions predicted between PER-2 and ceftazidime might explain the observed high catalytic efficiencies of PER  $\beta$ -lactamases toward ceftazidime (12, 13, 15). The observed differences in the kinetic behavior toward ceftazidime between PER-2 and PER-1 are probably due to the presence of differential residues like Arg240A (replaced by Lys in PER-1) and warrant further study.

Finally, inactivators like clavulanic acid might also be properly stabilized during inhibition (data not shown), based on models obtained by comparison with the structure of SHV-1 in complex with clavulanate (PDB 2H0T) (45). According to the models, Gln69, Arg220, Thr237, and probably Arg240A might be important in the stabilization of the clavulanate molecule.

In TEM and SHV  $\beta$ -lactamases with decreased susceptibility to inhibition by clavulanic acid, various mutations at Arg244 suggest that the interaction between this residue and the clavulanate car-

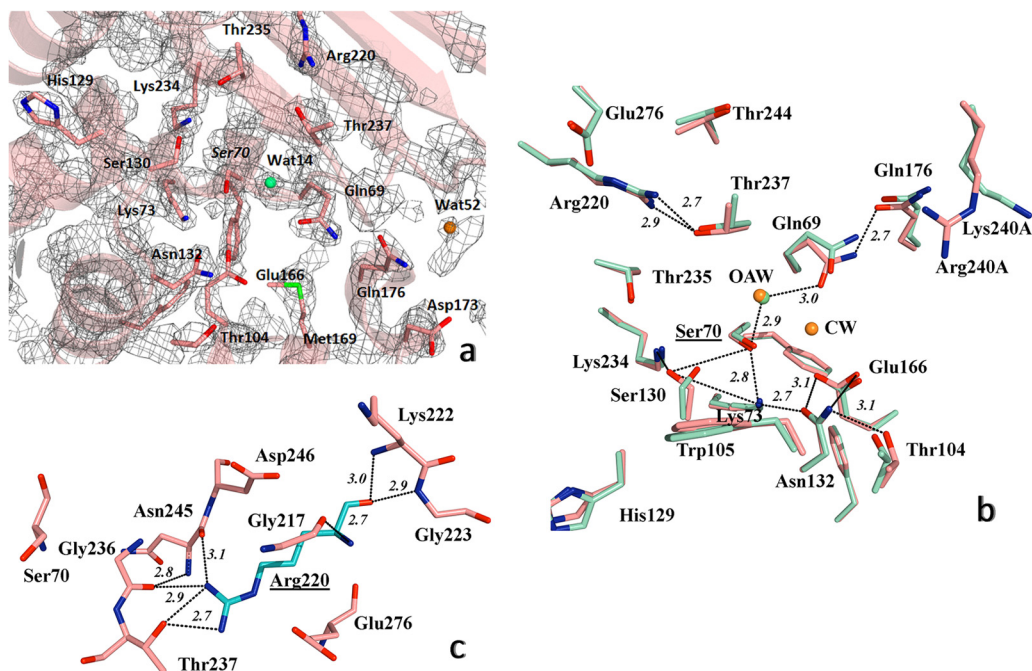


**FIG 3** Detailed view of the structure of active site of PER-2  $\beta$ -lactamase. (a) 2FoFc map contoured at 1.5 $\sigma$  is shown in gray around the most important amino acid residues within the active site; oxanion water molecule is shown as a green sphere, and additional water molecules in orange (see the Results and Discussion for details). (b) Comparative active site organization of PER-2 (pink) and PER-1 (cyan), indicating the main hydrogen bonds (black dashed lines) implicated in the stabilization of the active site of PER-2, including the oxanion water molecules (OAW) (green for PER-2 and orange for PER-1) and the catalytic water of PER-1 (CW) (orange), and the network Ser70-Gln69-Wat14-Thr237-Arg220 (see Results and Discussion for details); for visual convenience, only the hydrogen bonds for PER-2 were shown. (c) Position and occupancy of Arg220 in PER-2, allowing the creation of a unique network of hydrogen bonds with neighboring residues like Gly236, Thr237, Asn245, and Glu276, among others; Ser70 is shown as reference. Other color references: red, oxygen; blue, nitrogen; green, sulfur. All distances are in angstroms ( $\text{\AA}$ ).

boxylate is essential for clavulanate-mediated inactivation (35, 38, 46, 47).

In a recent publication, it was shown that clavulanate, upon acylation of the class A  $\beta$ -lactamase from *Bacillus licheniformis* BS3, generates two moieties, named CL1 (covalently linked to Ser70) and CL2 (48). According to comparative models with PER-2, both fragments might be in part associated by hydrogen bonds with residues like Gln69, Ser70, Ser130, and Thr237 (data not shown), if a similar inactivation mechanism actually occurs.

It has been previously reported that mutations at Gln69 do not seem to impair the inactivation by clavulanate (31). In addition, replacement of Arg220 or Thr237 seems to alter the behavior of PER-1 toward cephalosporins (13).

Preliminary results with different mutants of PER-2 in Arg220 have shown that modifications in this residue not only affect the susceptibility to inhibitors but also seem to impact the catalytic

behavior toward several antibiotics, especially cephalosporins (49).

As these residues appear to be important for the stabilization of the oxanion pocket, mutations in either of these residues probably affect the proper inactivation by mechanism-based inhibitors, probably by disrupting the integrity of the conserved hydrogen-bond network in which they participate.

In conclusion, extended-spectrum  $\beta$ -lactamase PER-2 is a unique enzyme from a structural point of view, belonging to a still small and not widely disseminated group of  $\beta$ -lactamases (seven members are now recognized) in which PER-1 and PER-2 represent the more frequently detected members.

We provided herein structural evidence of PER-2 suggesting that a previously not described hydrogen-bond network connecting Ser70-Gln69-water-Thr237-Arg220 is essential for the proper activity and inhibition of the enzyme.

**TABLE 2** Root mean square deviations between secondary structures and conserved motifs of PER-2 and other class A  $\beta$ -lactamases

$\beta$ -Lactamase	RMS deviation ( $\text{\AA}$ ) for:				
	Complete structure	SXXK motif	SDN motif	KTG motif	$\Omega$ loop
PER-1	0.619	0.116	0.128	0.016	0.220
TEM-1	1.810	0.118	0.086	0.081	3.453
SHV-1	1.894	0.182	0.048	0.033	3.308
TOHO-1	1.629	0.040	0.025	0.070	3.360
KPC-2	1.841	0.171	0.057	0.057	3.408

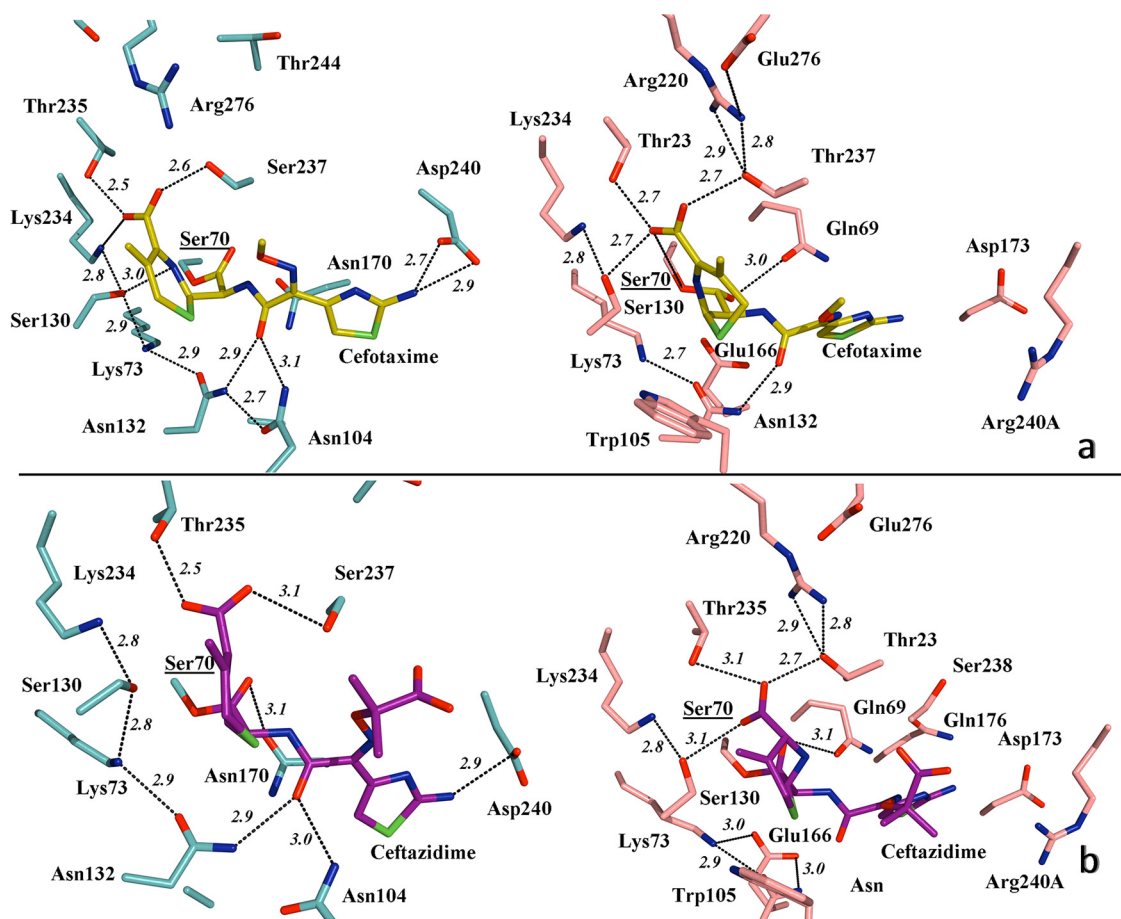


**FIG 4** (a) Detailed view of the active site of TOHO-1 (aqua) in association with cefotaxime (yellow) (left), indicating the main hydrogen bond interactions (PDB 1IYO), and simulated modeling of PER-2 (pink) and the probable positioning of cefotaxime within the active site (right), suggesting the putative most favorable hydrogen bonds and involvement of residues like Gln69, Thr237, and Arg240A in the stabilization of the oxymino-cephalosporin molecule. (b) Active site of TOHO-1 in complex with acylated ceftazidime (magenta) (left), indicating the main hydrogen bonds (PDB 2ZQD), compared to a simulated model of PER-2 and its probable association with ceftazidime (right), showing the predicted positioning of the molecule and the hydrogen bond interactions (black dashed lines). All distances are in angstroms (Å). Other color references: red, oxygen; blue, nitrogen; green, sulfur. See Results and Discussion for details.

We have also presented, through simulated models of PER-2 in association with oxymino-cephalosporins and clavulanate, the first evidence for the probable interactions of these  $\beta$ -lactams with key residues of the active site, proposing that residues like Gln69, Arg220, Thr237, and probably Asp173 and Arg240A, respectively, are important for the accommodation of  $\beta$ -lactams within, and their entrance into, the active site.

Our results provide a glimpse of hypothetically emerging mutants having disrupted hydrogen bond networks that display lower catalytic efficiencies toward some  $\beta$ -lactams (especially cephalosporins) and poorer inhibition by clavulanic acid.

Additional real structural models, complemented by kinetic data, will give us a more comprehensive understanding of the actual role of these residues in the high catalytic efficiency of PER-2 toward most  $\beta$ -lactams. In this regard, we foresee that mutations in either Arg220 (the counterpart of Arg244 in TEM/SHV variants) or Thr237 will probably result in more dramatic changes in the kinetic activity.

#### ACKNOWLEDGMENTS

This work was supported by grants from the University of Buenos Aires (UBACyT 2012-2015 [to P.P.] and 2011-2014 to [G.G.]), Con-

sejo Nacional de Investigaciones Científicas y Técnicas (CONICET PIP 2010-2012 [to P.P.]), Agencia Nacional de Promoción Científica y Tecnológica (BID PICT 2011-0742 [to G.G.]), and the Fonds de la Recherche Scientifique (IISN 4.4505.09, IISN 4.4509.11, and FRFC 2.4511.06F), by the Belgian Program on Interuniversity Poles of Attraction initiated by the Belgian State, Prime Minister's Office, Science Policy programming (IAP numbers P6/19 and P7/44), by the University of Liège (Fonds Spéciaux, Crédit Classique, C-06/19 and C-09/75), and by a bilateral scientific agreement (V4/325C) between the Belgian Funds for Scientific Research (FRS-FNRS) (to M.G.) and the Consejo Nacional de Investigaciones Científicas y Técnicas (CONICET) (to G.G. and later to P.P.).

M. Ruggiero is a Ph.D. fellow for the Consejo Nacional de Investigaciones Científicas y Técnicas (CONICET, Argentina) and was a recipient of an Alfa-Bacterialnet doctoral visiting fellowship at the CIP (U. Liege). P. Power and G. Gutkind are researchers for the CONICET, Argentina. F. Kerff is an associate researcher for the Fonds de la Recherche Scientifique (FNRS, Belgium).

We thank the staff of Proxima1 beamline at Soleil synchrotron for assistance in X-ray data collection and Nicole Otthiers, Anne-Marie Matton, and Fabrice Bouillenne (CIP, University of Liege, Belgium) for their precious assistance in the N-terminal determination and  $\beta$ -lactamase purification process.

## REFERENCES

- Bush K, Jacoby GA. 2010. Updated functional classification of  $\beta$ -lactamases. *Antimicrob. Agents Chemother.* 54:969–976. <http://dx.doi.org/10.1128/AAC.01009-09>.
- Gutkind GO, Di Conza J, Power P, Radice M. 2013.  $\beta$ -Lactamase-mediated resistance: a biochemical, epidemiological and genetic overview. *Curr. Pharm. Des.* 19:164–208. <http://dx.doi.org/10.2174/138161213804070320>.
- Nordmann P, Ronco E, Naas T, Dupont C, Michel-Briand Y, Labia R. 1993. Characterization of a novel extended-spectrum  $\beta$ -lactamase from *Pseudomonas aeruginosa*. *Antimicrob. Agents Chemother.* 37:962–969. <http://dx.doi.org/10.1128/AAC.37.5.962>.
- Vahaboglu H, Dodanlı S, Eroglu C, Ozturk R, Soyletir G, Yildirim I, Avkan V. 1996. Characterization of multiple-antibiotic-resistant *Salmonella* Typhimurium stains: molecular epidemiology of PER-1-producing isolates and evidence for nosocomial plasmid exchange by a clone. *J. Clin. Microbiol.* 34:2942–2946.
- Vahaboglu H, Ozturk R, Aygun G, Coskuncan F, Yaman A, Kaygusuz A, Leblebicioglu H, Balik I, Aydin K, Otkun M. 1997. Widespread detection of PER-1-type extended-spectrum  $\beta$ -lactamases among nosocomial *Acinetobacter* and *Pseudomonas aeruginosa* isolates in Turkey: a nationwide multicenter study. *Antimicrob. Agents Chemother.* 41:2265–2269.
- Poirel L, Karim A, Mercat A, Le Thomas I, Vahaboglu H, Richard C, Nordmann P. 1999. Extended-spectrum  $\beta$ -lactamase-producing strain of *Acinetobacter baumannii* isolated from a patient in France. *J. Antimicrob. Chemother.* 43:157–158. <http://dx.doi.org/10.1093/jac/43.1.157>.
- Bonnin RA, Potron A, Poirel L, Lecuyer H, Neri R, Nordmann P. 2011. PER-7, an extended-spectrum  $\beta$ -lactamase with increased activity toward broad-spectrum cephalosporins in *Acinetobacter baumannii*. *Antimicrob. Agents Chemother.* 55:2424–2427. <http://dx.doi.org/10.1128/AAC.01795-10>.
- Rossi MA, Gutkind G, Quinteros M, Marino E, Couto E, Tokumoto M, Woloj M, Miller G, Medeiros A. 1991. A *Proteus mirabilis* with a novel extended spectrum  $\beta$ -lactamase and six different aminoglycoside resistance genes, abstr 939, p 255. Abstr. 31st Intersc. Conf. Antimicrob. Agents Chemother. American Society for Microbiology, Washington, DC.
- Bauernfeind A, Stemplinger I, Jungwirth R, Mangold P, Amann S, Akalin E, Ang O, Bal C, Casellas JM. 1996. Characterization of  $\beta$ -lactamase gene *bla*<sub>PER-2</sub>, which encodes an extended-spectrum class A  $\beta$ -lactamase. *Antimicrob. Agents Chemother.* 40:616–620.
- Quinteros M, Radice M, Gardella N, Rodríguez MM, Costa N, Korbenfeld D, Couto E, Gutkind G, The Microbiology Study Group. 2003. Extended-spectrum  $\beta$ -lactamases in *Enterobacteriaceae* in Buenos Aires, Argentina, public hospitals. *Antimicrob. Agents Chemother.* 47:2864–2869. <http://dx.doi.org/10.1128/AAC.47.9.2864-2867.2003>.
- Girlich D, Poirel L, Nordmann P. 2010. PER-6, an extended-spectrum  $\beta$ -lactamase from *Aeromonas allosaccharophila*. *Antimicrob. Agents Chemother.* 54:1619–1622. <http://dx.doi.org/10.1128/AAC.01585-09>.
- Power P, Di Conza J, Rodriguez MM, Ghiglione B, Ayala JA, Casellas JM, Radice M, Gutkind G. 2007. Biochemical characterization of PER-2 and genetic environment of *bla*<sub>PER-2</sub>. *Antimicrob. Agents Chemother.* 51:2359–2365. <http://dx.doi.org/10.1128/AAC.01395-06>.
- Bouthors AT, Delette J, Mugnier P, Jarlier V, Sougakoff W. 1999. Site-directed mutagenesis of residues 164, 170, 171, 179, 220, 237 and 242 in PER-1  $\beta$ -lactamase hydrolysing expanded-spectrum cephalosporins. *Protein Eng.* 12:313–318. <http://dx.doi.org/10.1093/protein/12.4.313>.
- Tranier S, Bouthors AT, Maveyraud L, Guillet V, Sougakoff W, Samama JP. 2000. The high-resolution crystal structure for class A  $\beta$ -lactamase PER-1 reveals the bases for its increase in breadth of activity. *J. Biol. Chem.* 275:28075–28082. <http://dx.doi.org/10.1074/jbc.M003802200>.
- Bouthors AT, Dagoneau-Blanchard N, Naas T, Nordmann P, Jarlier V, Sougakoff W. 1998. Role of residues 104, 164, 166, 238 and 240 in the substrate profile of PER-1  $\beta$ -lactamase hydrolysing third-generation cephalosporins. *Biochem. J.* 330:1443–1449.
- Hansen JB, Olsen RH. 1978. Isolation of large bacterial plasmids and characterization of the P2 incompatibility group plasmids pMG1 and pMG5. *J. Bacteriol.* 135:227–238.
- Power P, Radice M, Barberis C, de Mier C, Mollerach M, Maltagliatti M, Vay C, Famiglietti A, Gutkind G. 1999. Cefotaxime-hydrolysing  $\beta$ -lactamases in *Morganella morganii*. *Eur. J. Clin. Microbiol. Infect. Dis.* 18:743–747. <http://dx.doi.org/10.1007/s100960050391>.
- Kabsch W. 2010. XDS. *Acta Crystallogr. D Biol. Crystallogr.* 66:125–132. <http://dx.doi.org/10.1107/S0907444909047337>.
- Kabsch W. 2010. Integration, scaling, space-group assignment and postrefinement. *Acta Crystallogr. D Biol. Crystallogr.* 66:133–144. <http://dx.doi.org/10.1107/S0907444909047374>.
- Murshudov GN, Vagin AA, Dodson EJ. 1997. Refinement of macromolecular structures by the maximum-likelihood method. *Acta Crystallogr. D Biol. Crystallogr.* 53:240–255. <http://dx.doi.org/10.1107/S0907444996012255>.
- Painter J, Merritt EA. 2006. Optimal description of a protein structure in terms of multiple groups undergoing TLS motion. *Acta Crystallogr. D Biol. Crystallogr.* 62:439–450. <http://dx.doi.org/10.1107/S0907444906005270>.
- Emsley P, Cowtan K. 2004. Coot: model-building tools for molecular graphics. *Acta Crystallogr. D Biol. Crystallogr.* 60:2126–2132. <http://dx.doi.org/10.1107/S0907444904019158>.
- Schrödinger. The PyMOL molecular graphics system, version 1.5.0.4. Schrödinger, Portland, OR.
- Shimamura T, Ibuka A, Fushinobu S, Wakagi T, Ishiguro M, Ishii Y, Matsuzawa H. 2002. Acyl-intermediate structures of the extended-spectrum class A  $\beta$ -lactamase, Toho-1, in complex with cefotaxime, cephalothin, and benzylpenicillin. *J. Biol. Chem.* 277:46601–46608. <http://dx.doi.org/10.1074/jbc.M207884200>.
- Padayatti PS, Helfand MS, Totir MA, Carey MP, Carey PR, Bonomo RA, van den Akker F. 2005. High resolution crystal structures of the trans-enamine intermediates formed by sulbactam and clavulanic acid and E166A SHV-1  $\beta$ -lactamase. *J. Biol. Chem.* 280:34900–34907. <http://dx.doi.org/10.1074/jbc.M505333200>.
- Krieger E, Darden T, Nabuurs SB, Finkelstein A, Vriend G. 2004. Making optimal use of empirical energy functions: force-field parameterization in crystal space. *Proteins* 57:678–683. <http://dx.doi.org/10.1002/prot.20251>.
- Krieger E, Joo K, Lee J, Raman S, Thompson J, Tyka M, Baker D, Karplus K. 2009. Improving physical realism, stereochemistry, and side-chain accuracy in homology modeling: four approaches that performed well in CASP8. *Proteins* 77:114–122. <http://dx.doi.org/10.1002/prot.22570>.
- Essmann U, Perera L, Berkowitz ML, Darden T, Lee H, Pedersen LG. 1995. A smooth particle mesh Ewald method. *J. Chem. Phys.* 103:8577–8593. <http://dx.doi.org/10.1063/1.470117>.
- Pal D, Chakrabarti P. 1998. Different types of interactions involving cysteine sulfhydryl group in proteins. *J. Biomol. Struct. Dyn.* 15:1059–1072. <http://dx.doi.org/10.1080/07391102.1998.10509001>.
- Tatko CD, Waters ML. 2004. Investigation of the nature of the methionine-pi interaction in  $\beta$ -hairpin peptide model systems. *Protein Sci.* 13:2515–2522. <http://dx.doi.org/10.1110/ps.04820104>.
- Bouthors AT, Jarlier V, Sougakoff W. 1998. Amino acid substitutions at positions 69, 165, 244 and 275 of the PER-1  $\beta$ -lactamase do not impair enzyme inactivation by clavulanate. *J. Antimicrob. Chemother.* 42:399–401.
- Chen CC, Herzberg O. 1999. Relocation of the catalytic carboxylate group in class A  $\beta$ -lactamase: the structure and function of the mutant enzyme Glu166→Gln:Asn170→Asp. *Protein Eng.* 12:573–579. <http://dx.doi.org/10.1093/protein/12.7.573>.
- Zawadzke LE, Chen CC, Banerjee S, Li Z, Wasch S, Kapadia G, Moulton J, Herzberg O. 1996. Elimination of the hydrolytic water molecule in a class A  $\beta$ -lactamase mutant: crystal structure and kinetics. *Biochem. J.* 35:16475–16482. <http://dx.doi.org/10.1021/bi962242a>.
- Bret L, Chaibi EB, Chanal-Claris C, Sirot D, Labia R, Sirot J. 1997. Inhibitor-resistant TEM (IRT)  $\beta$ -lactamases with different substitutions at position 244. *Antimicrob. Agents Chemother.* 41:2547–2549.
- Thomson JM, Distler AM, Prati F, Bonomo RA. 2006. Probing active site chemistry in SHV  $\beta$ -lactamase variants at Ambler position 244. Understanding unique properties of inhibitor resistance. *J. Biol. Chem.* 281:26734–26744. <http://dx.doi.org/10.1074/jbc.M603222200>.
- Moews PC, Knox JR, Dideberg O, Charlier P, Frere JM. 1990.  $\beta$ -Lactamase of *Bacillus licheniformis* 749/C at 2 Å resolution. *Proteins* 7:156–171. <http://dx.doi.org/10.1002/prot.340070205>.
- Perez-Llarena FJ, Cartelle M, Mallo S, Becerro A, Perez A, Villanueva R, Romero A, Bonnet R, Bou G. 2008. Structure-function studies of arginine at position 276 in CTX-M  $\beta$ -lactamases. *J. Antimicrob. Chemother.* 61:792–797. <http://dx.doi.org/10.1093/jac/dkn031>.
- Marciano DC, Brown NG, Palzkill T. 2009. Analysis of the plasticity of location of the Arg244 positive charge within the active site of the TEM-1



- $\beta$ -lactamase. *Protein Sci.* 18:2080–2089. <http://dx.doi.org/10.1002/pro.220>.
39. Jacob-Dubuisson F, Lamotte-Brasseur J, Dideberg O, Joris B, Frere JM. 1991. Arginine 220 is a critical residue for the catalytic mechanism of the *Streptomyces albus* G  $\beta$ -lactamase. *Protein Eng.* 4:811–819. <http://dx.doi.org/10.1093/protein/4.7.811>.
  40. Papp-Wallace KM, Taracila MA, Smith KM, Xu Y, Bonomo RA. 2012. Understanding the molecular determinants of substrate and inhibitor specificity in the carbapenemase KPC-2: exploring the roles of Arg220 and Glu276. *Antimicrob. Agents Chemother.* 56:4428–4438. <http://dx.doi.org/10.1128/AAC.05769-11>.
  41. Matagne A, Frere JM. 1995. Contribution of mutant analysis to the understanding of enzyme catalysis: the case of class A  $\beta$ -lactamases. *Biochim. Biophys. Acta* 1246:109–127. [http://dx.doi.org/10.1016/0167-4838\(94\)00177-1](http://dx.doi.org/10.1016/0167-4838(94)00177-1).
  42. Delmas J, Leysse D, Dubois D, Birck C, Vazeille E, Robin F, Bonnet R. 2010. Structural insights into substrate recognition and product expulsion in CTX-M enzymes. *J. Mol. Biol.* 400:108–120. <http://dx.doi.org/10.1016/j.jmb.2010.04.062>.
  43. Raquet X, Lamotte-Brasseur J, Fonze E, Goussard S, Courvalin P, Frere JM. 1994. TEM  $\beta$ -lactamase mutants hydrolysing third-generation cephalosporins. A kinetic and molecular modelling analysis. *J. Mol. Biol.* 244: 625–639.
  44. Ibuka AS, Ishii Y, Galleni M, Ishiguro M, Yamaguchi K, Frere JM, Matsuzawa H, Sakai H. 2003. Crystal structure of extended-spectrum  $\beta$ -lactamase Toho-1: insights into the molecular mechanism for catalytic reaction and substrate specificity expansion. *Biochem. J.* 42:10634–10643. <http://dx.doi.org/10.1021/bi0342822>.
  45. Totir MA, Padayatti PS, Helfand MS, Carey MP, Bonomo RA, Carey PR, van den Akker F. 2006. Effect of the inhibitor-resistant M69V substitution on the structures and populations of trans-enamine  $\beta$ -lactamase intermediates. *Biochem.* 45:11895–11904. <http://dx.doi.org/10.1021/bi060990m>.
  46. Belaouaj A, Lapoumeroulie C, Canica MM, Vedel G, Nevot P, Krishnamoorthy R, Paul G. 1994. Nucleotide sequences of the genes coding for the TEM-like  $\beta$ -lactamases IRT-1 and IRT-2 (formerly called TRI-1 and TRI-2). *FEMS Microbiol. Lett.* 120:75–80.
  47. Giakkoupi P, Tzelepi E, Legakis NJ, Tzouveleki LS. 1998. Substitution of Arg-244 by Cys or Ser in SHV-1 and SHV-5  $\beta$ -lactamases confers resistance to mechanism-based inhibitors and reduces catalytic efficiency of the enzymes. *FEMS Microbiol. Lett.* 160:49–54.
  48. Power P, Mercuri P, Herman R, Kerff F, Gutkind G, Dive G, Galleni M, Charlier P, Sauvage E. 2012. Novel fragments of clavulanate observed in the structure of the class A  $\beta$ -lactamase from *Bacillus licheniformis* BS3. *J. Antimicrob. Chemother.* 67:2379–2387. <http://dx.doi.org/10.1093/jac/dks231>.
  49. Ruggiero M, Sauvage E, Troncoso F, Curto L, Galleni M, Power P, Gutkind G. 2012. Mutations in R220 in PER-2  $\beta$ -lactamase resulting in a decreased susceptibility to inhibitors also impact in the catalytic activity towards substrates, abstr C1-1206, p 134. Abstr. 52nd Intersci. Conf. Antimicrob. Agents Chemother. American Society for Microbiology, Washington, DC.